Journal of Engineering and Sustainable Development
Vol. 30, No. 05, August 2026
https://jeasd.uomustansiriyah.edu.iq/index.php/jeasd
ISSN 2520-0917
Research Article
https://doi.org/10.31272/jeasd.3970

Removal of Pyridine from Aqueous Solutions by Adsorption Using Tangerine Peels: Operating and Morphological Studies

Nadia Matter Almhana[1*], Zainab A. Naser[1], Manar Banwan Hasan[1], Marwan Arkan Hussein[1], Israa M. Al-Tameemi[2], Ola Tareq al-Hussain[2]

[1]Environmental Engineering Department, College of Engineering, Mustansiriyah University, Baghdad, Iraq
[2]School of Civil Engineering, Universiti Sains Malaysia, Penang 14300, Malaysia

[*]Email: nadia.almhana@uomustansiriyah.edu.iq

Article Info

Received	**06/03/2026**
Revised	**30/06/2026**
Accepted	**30/06/2026**

Abstract

The current study focuses on the utilization of tangerine peels, a major agricultural waste generated by consuming this fruit, as a low-cost adsorbent for removing pyridine from contaminated aqueous solutions. The adsorption performance was assessed through batch adsorption tests conducted under various operational conditions. The study reported that tangerine peels had a high capacity for the removal of pyridine, the maximum pyridine removal efficiency reached 83.6% under optimized operating conditions, including an adsorbent dosage of 5.8 g, pH 6, agitation speed of 400 rpm, and contact time of 150 min, where efficiency increased as agitation speed, adsorbent dose and contact time were raised, but decreased with greater values for other variables. pH left runs with pyridine removal both increased in the acidic range to pH 6; however, they decreased under neutral and alkaline conditions. Morphological study indicated that the surface area reduced from 16 to 3.25 m²/g after adsorption of tangerine peels. The occupation of active sites and depletion of functional groups on the adsorbent surface were further confirmed with Fourier Transform Infrared Spectroscopy (FTIR) analysis, whereas Field Emission Scanning Electron Microscopy (FESEM) images showed clear surface changes post-adsorption.

Keywords: Adsorption, Batch Unit, Pyridine, Removal, Tangerine Peels.

1. Introduction

The issue of water pollution by synthetic organic compounds has a unique place of risk and intricacy. These compounds, mainly resulting from the petrochemical, pharmaceutical, and agricultural industries, include many categories such as halide solvents, such as chloroform and tetrachloroethylene, polycyclic aromatic hydrocarbons (PAHs), phthalates, organochlorine and organophosphorus pesticides, and dioxins [1]. These pollutants reach water bodies through various routes, the most important of which are direct industrial wastewater leak discharges, landfill leachate, and agricultural surface runoff carrying pesticide residues and toxic fertilizers [2]. What distinguishes many of these compounds is the property of "environmental stability," that is, their resistance to biological, chemical, or photochemical degradation under natural environmental conditions, which enables them to remain for long periods of time, travel long distances from their original source, accumulate in the fatty tissues of living organisms through a process known as bioaccumulation, and increase in concentration across the food chain in the phenomenon of biomagnification [3]. This condition results in cumulative health and environmental risks, including acute and chronic toxicity to aquatic organisms, carcinogenic, teratogenic, and anti-endocrine effects on mammals and humans, and long-term degradation of aquatic habitat quality [4]. Pyridine is an example of the persistent and toxic industrial organic pollutant amidst this general and alarming class of organic pollutants [5]. Chemically, pyridine is a six-membered ring heterocyclic aromatic compound, with the chemical formula C5H5N, in which one nitrogen atom replaces the CH-group in the benzene ring [6]. A graduated pyridine color under laboratory conditions is recognized as a change from a clear to a pale yellow liquid with a sharp, foul smell resembling rotting fish, detectable by the human nose at very low concentrations, down to about 0.1 ppm [7]. The base is fully miscible in water and most common organic solvents (ethanol, ether, chloroform), a quality that enhances the rapid dissemination of the compound into aqueous environments and possesses a density of 0.982 g/mL, a boiling

point of 115.2 °C, and a melting point of −41.6 °C [8]. In terms of chemical functionality, pyridine can be classified as a weak organic base (pKa ≈ 5.25); hence, it can accept a proton to become a positive pyridinium ion under acidic conditions, and this determines its properties under a range of pH conditions in water and during adsorption treatment systems [8]. The environmental hazard of pyridine stems from the widespread use of its multiple industrial applications, which make it a vital intermediate in many manufacturing chains [8]. Its first and most important use is as an excellent solvent in chemical reactions, especially those that require an alkaline medium that is miscible with water [9]. However, its greatest environmental impact stems from its use as an essential intermediate compound in the manufacture of a vast array of products. In the agricultural sector [10], Pyridine is an important substance in the preparation of some highly toxic and widely used insecticides, fungicides, and herbicides, such as Paraquat (N, N′-dimethyl-4,4′-bipyridinium dichloride, of a chemical formula (C6H7N)2Cl2), which is known for its extreme toxicity to humans, and Dichlorvos (2,2-Dichlorovinyl dimethyl phosphate, of a chemical formula C4H7Cl2O4P). It is also used in the formulation of corrosion inhibitors for drilling fluids in the oil and gas industry [11]. In the pharmaceutical industry, pyridine is a necessary raw material for the preparation of many drugs and medications, such as antihistamines, antibacterial drugs such as sulfonamides (C22H23N3O5S), vitamins such as niacin (vitamin B3), and stimulants [12]. Such widespread industrial dispersion leads to an environmental issue of persistent pyridine contamination when significant amounts of this compound enter various environmental compartments, primarily water; this occurs through several major pathways, especially the effluents from factories where this base is employed in production or used as a solvent that usually do not possess treatment specifically for this compound; accidental leaks during transport or storage; and leaching from industrial waste landfills with pyridine-containing products or wastes [13]. Field data from various regions globally, particularly near industrial chemical complexes or pharmaceutical production facilities, have shown surface and groundwater contamination with pyridine of a few µg/l to several hundred µg/l [14]. The problem is that pyridine is highly soluble in water, easily transported, and not precipitated. Moreover, its stability (so-called resistance against rapid biodegradation, especially under aerobic circumstances), as well as its unique resistance to biodegradation (essentially persistence), contributes to its extended persistence in the environment and its increased likelihood of exposure to living organisms [15]. This risk means that global water quality standards and guidelines set very low maximum concentrations of pyridine, significantly lower than the concentrations recorded in this study [16]. As an example, although the United States Environmental Protection Agency (EPA) has not established a formal Maximum Contaminant Level for pyridine in drinking water, the Occupational Safety and Health Administration (OSHA) has set a permissible exposure limit of 5 ppm as an 8-hour time-weighted average in air, reflecting the recognized toxicity of this compound even at low concentrations [17]. Long-term effects from chronic exposure at low concentrations (as in drinking water contamination cases) culminate in severe organ toxicity, including irreversible liver and kidney injury leading to organ failure [18]. It is categorized by the International Agency for Research on Cancer (IARC) as a "possible human carcinogen" (Group 2B), based on sufficient evidence for carcinogenicity in rodent studies and sufficient evidence of its effect on fertility and embryonic development; in addition, it produces various neurological disorders, including peripheral nerve damage and mood and memory disorders [16]. Although several techniques are available for the removal of pyridine, the most commonly employed method is adsorption using adsorbents with high surface area and small pore channels to capture pyridine molecules [19]. Conventional activated carbon is relatively very effective, but research has focused on modified or hybrid adsorbent materials to enhance capacity and selectivity, e.g., chemically treated charcoal, zeolite, or hybrids of zeolites or nanomaterials such as nanometal oxides or carbon nanotubes onto a wide range of supports [20]. Adsorption efficacy is strongly influenced by the operating conditions, such as pH, which affects the surface charge of the adsorbent and the pyridine form (neutral or pyridinium ion) [21]. Advanced oxidation is another novel method that targets the destruction of pyridine through photochemical or chemical degradation into harmless intermediate degradation products followed by ultimate degradation to carbon dioxide and water [22]. These processes involve ozone (O3) with or without ultraviolet radiation or hydrogen peroxide (H2O2), photo-Fenton processes with iron ions and UV/H2O2 radiation [22], where semiconductor catalysts like titanium dioxide (TiO2) are used in photocatalysis processes [23]. These approaches suffer from the risk of generating toxic intermediate species, rendering the precise control of reaction conditions mandatory. Previous studies have reported that pyridine concentrations in industrial wastewater commonly range from 20–300 mg/L, while accidental or emergency industrial discharges may increase these concentrations to 600 mg/L or more, posing significant environmental and human health risks due to pyridine's toxicity, persistence, and resistance to biodegradation. Investigated the adsorption of pyridine from simulated wastewater using coke powder as a low-cost adsorbent and reported promising removal performance under optimized operating conditions. While the use of agricultural waste is gaining attention as a cheap adsorbent for wastewater treatment, few studies have focused on tangerine peels' capacity to remove pyridine from aqueous solutions. The current study investigates the effectiveness of tangerine peels as a low-cost and abundant agricultural waste-based adsorbent for removing pyridine using a batch adsorption system under varying operational conditions, namely pH, initial concentration of pyridine, agitation speed, amount of adsorbent, and temperature. Likewise, waste mandarin peel-derived biochar exhibited promising adsorption efficiency and high surface activity for wastewater treatment applications. In addition, recent investigations confirmed that tangerine peel-derived adsorbents possess suitable porous morphology and abundant active sites, making them promising eco-friendly materials for pollutant removal from contaminated aqueous systems [24]. The novelty of this study compared to other related ones is that it investigates the use of untreated tangerine peels as a potential sustainable adsorbent and explores their adsorption performance, accompanied by detailed morphological characterization. This study aims to promote an environmentally benign and economically viable

methodology for the treatment of water polluted with pyridine while facilitating the understanding of structural changes of the adsorbent upon adsorption through Scanning Electron Microscopy (SEM), Brunauer–Emmett–Teller) BET analysis, and FTIR.

2. Method of the Research

2.1. Materials Used

Double-distilled water was obtained from a laboratory distillation system with an electrical conductivity of EC=2.2 µs/cm at 25 °C. High-purity (≥ 99%) pyridine base (C5H5N) with a molecular weight of 79.01 mol/g, used in the preparation of the stock solution and experimental solutions, was purchased from MIVON CHEMICALS, India, as a white powder with a strong, unpleasant, fish-like odor. Colorless and odorless 0.1% normal concentration solutions of hydrochloric acid (pH ≈ 1.0–1.2) and sodium hydroxide (pH ≈ 12–13) were obtained from Bharad Fine Chemicals Industries Pvt. Ltd. and Loba Chemie, India, respectively. The medical alcohol used for sterilizing various equipment and instruments was of 99% purity and was supplied by SLC Chemicals, India. Different pyridine concentrations were used throughout the experimental program depending on the objective of each adsorption parameter study. Lower concentrations (1 mg/L) were employed during pH and agitation speed investigations to assess the sensitivity of adsorption behavior under dilute conditions, whereas higher concentrations (96 mg/L) were selected for dosage, contact time, and thermodynamic studies to better evaluate adsorption capacity and adsorbent performance under more challenging pollutant-loading conditions.

2.2. Equipment and Devices Used

The Digital Water Bath Shaker used was of the SHKA7000 model, Thermo-Fischer, USA, while the pyridine concentration was measured using a UV-Vis device, SPECORD®:200 Plus, Analytik Jena, Germany. A Benchtop pH Meter (Inno-PH18, Inno Tech Technologies, USA) was used. The magnetic stirrer hot plate was of type H3770-GROUP – Benchmark Scientific, Inc., USA. The laboratory distillation apparatus (single distillation Glass Water Still) producing double-distilled water with a capacity of 8 L/h was of type GLF-2208, Lauda, Germany. To determine the masses of the different materials, a sensitive digital electronic weight scale (JA103P, FAITHFUL, China) was used. The virgin hollyhock peels were ground using a laboratory grinder (RRH-100, RIRIHONG, China). The oven used to dry the samples was a B-30 Memmert (Germany type, while the samples were filtered after adsorption using Whatman 40 filter paper, and the separation process was completed using a Vacuum Filtration Kit-2 type EIS-CH200501, CP Lab Safety, China. The sieving process of virgin tangerine peel powder was carried out using a reproducible sieve analysis of the type Sieve Shaker AS 200 tap – Retsch, Germany. The morphological examinations were performed using several devices, including the (BELSORP MR1, Microtrac Company, USA) device for measuring surface area, the (IRSpirit-X Series, Shimadzu, Japan) device used for identifying the functional groups on the surface of the adsorbent material via Fourier transform infrared (FTIR) analysis, and the (FlexSEM 1000 II, Hitachi High-Tech, Japan) device for identifying Field emission scanning electron microscopy (FESEM). All Pyrex lab glassware used in this investigation, including flasks, funnels, volumetric bottles, conical flasks, and beakers, was supplied by BOROSIL® Scientific Company, India. The 500ml amber jars used were supplied by Pack My Product, Adelaide, Australia.

2.3 Tangerine Peels

The current study used the tangerine peels of Egyptian origin, which represent one of the types of citrus waste available year-round, as a low-cost, non-valuable absorbent material. The required tangerine peels were collected from household consumption and manually peeled prior to washing and drying procedures. Each collected batch of peels was washed with excess tap water and liquid soap – as a first step – to remove any impurities or dirt. This was followed by rinsing the peels with double-distilled water to ensure they were clean and suitable for laboratory work. The clean peels were spread out in aluminum metal trays for outdoor drying at a temperature between 17 and 20 °C for 5 days, at a rate of 10 hours per day. Finally, they were dried in an electric drying oven for 6 h at 70 °C to achieve weight equilibrium without carborizing and changing their structural nature. The dried peels were powdered with a laboratory grinder until a fine powder was obtained and sieved through a series of sieves in different diameters. Among those peels passing through the 10-mesh sieve, it was chosen because it had the highest yield ratio. The selected peels were placed in dark amber glass jars with tight-sealing lids wrapped in a layer of aluminum foil, and maintained in clean and dry conditions at ≤ 4 °C until use.

2.4. Stock Solution of Pyridine

In order to avoid the interference of pipetting multiple contaminants contained in real water on the test results, and to accurately test the ability of the adsorbent to remove target bases, the performance of tangerine peels as an adsorbent for pyridine using a pre-prepared solution with a certain concentration of pyridine was studied. In preparing these solutions, a stock solution of pyridine at a known concentration must be diluted in varying volumes to obtain the concentrations necessary for study. A stock solution was prepared as follows: 1 g of the organic pyridine base, measured on a theoretical balance, was dissolved in a beaker of a definite volume, along with a few drops of double-distilled water, as described in [20]. The dissolution process was carried out using a magnetic stirrer hot plate at 100 rpm for 15 minutes at laboratory temperature to achieve complete dissolution. After confirming that the pyridine mass has dissolved, it is carefully transferred to a clean, sterile 1000 mL volumetric flask using a clean, sterile glass funnel, and the volume is topped up to the indicated mark with double-distilled water. The volumetric flask is wrapped in aluminum foil and stored in a clean, dry place, away from light and sunlight. Each 1 mL of the prepared stock solution contains 1 mg of pyridine.

2.5. Calibration Curve

It is a fundamental quantitative analytical tool in analytical chemistry experiments, including adsorption. It is used to convert the response of a spectrophotometer into a digitally

measurable signal of the concentration of the substance to be removed in the sample. It is constructed experimentally by preparing a series of standard solutions with known and graded concentrations of the target substance, then measuring and recording the response signal from the analyzer for each standard solution. Then, the pollutant concentration (on the x-axis) is plotted against the corresponding response signal (on the y-axis) to obtain a series of points that are statistically fitted to generate a statistically linear function describing the relationship between the two variables (y=mx+b, where m represents the slope of the curve and b is the y-intercept). A good curve should be linear; the closer the correlation coefficient R2 is to 1, the higher the accuracy [25]. When analyzing a sample of unknown concentration, resulting from treating solutions of known concentration with the adsorbent under specific operating conditions, its signal is measured as a response, and the calibration curve equation is applied to accurately calculate the concentration of the residual substance, taking into account the margin of error. In the current study, solutions of known concentration of pyridine were prepared, and the response of the UV-Vis device was measured for each concentration in triplicate. From the resulting data, the calibration curve used in the current study is derived, as shown in Fig. 1.

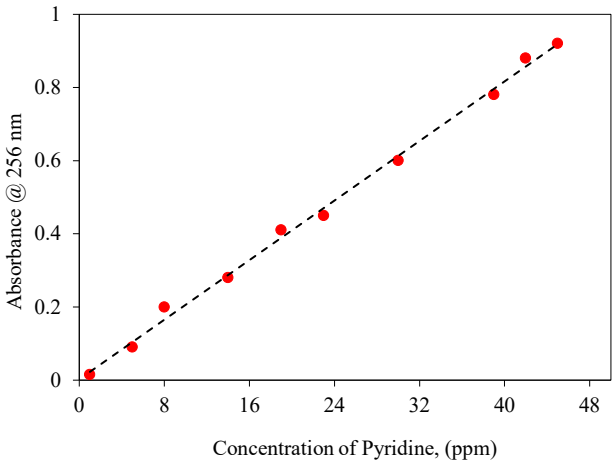

Figure 1. UV-Vis Calibration curve of pyridine used in this study.

2.6. Batch Adsorption Unit

A batch adsorption unit is a laboratory system designed to study the adsorption process to remove contaminants from the liquid or gaseous phase by adhering them onto the surface of a solid adsorbent material. The mechanism of action relies on placing a specific quantity of the adsorbent inside a glass flask after adding a calculated volume of liquid solution containing the target (adsorbed) substance at a known concentration and pH. The mixture is continuously stirred at a selected temperature, either by a magnetic agitator or a mechanical vibrator, to ensure adequate contact and efficient diffusion of the material towards the adsorption sites on the inner surface of the adsorbent material. This unit aims to measure the performance of the adsorbent by tracking the change in the concentration of the pollutant over time until it reaches equilibrium, providing important data for calculating the maximum adsorption capacity, mass transfer rate, nature of surface reaction mechanisms, and kinetic, isothermal, and thermodynamic model parameters. Experiments were conducted to investigate the performance of virgin tangerine peels in removing pyridine from contaminated solutions using a shaking water bath and under different operating conditions: contact time, initial concentration of the target substance, temperature, agitation speed, dosage of adsorbent, and pH of the contaminated solution. The ranges of the studied parameters were 10–180 minutes, 1–100 ppm, 25–50 °C, 100–500 rpm, 0.5–6 g, and 1–9, respectively. The final pyridine concentration after treatment was determined spectroscopically using a correction curve, while the removal efficiency and virgin linseed recovery capacity were calculated using (1) and (2), respectively [19].

$$\%E = \frac{C_i - C_e}{C_i} \quad (1)$$

$$q = \frac{V}{w}(C_i - C_e) \quad (2)$$

Where: %E: the percent adsorption efficiency (-), q: capacity of virgin tangerine peels for pyridine adsorption (mg/g), V: volume of solution used in the experiment (0.1 L), w: mass of linkins used in the experiment, which ranges between (0.5 – 6.0 g), C_i: pyridine concentration before the adsorption process (ppm), C_e: pyridine concentration after the adsorption process (ppm).

2.7. Thermodynamic Study

The thermodynamic behavior of pyridine adsorption onto tangerine peels was evaluated using Van't Hoff analysis to determine the changes in Gibbs free energy (ΔG°), enthalpy (ΔH°), and entropy (ΔS°). The thermodynamic parameters were calculated using the following:

$$Ce = Ci\,(1 - \frac{\%E}{100}) \quad (3)$$

$$Kc = \frac{C_i - C_e}{C_e} \quad (4)$$

$$Ln\,Kc = -\frac{\Delta H^o}{RT} + \frac{\Delta S^o}{R} \quad (5)$$

$$\Delta G^o = \Delta H^o - T\Delta S^o \quad (6)$$

Or $$\Delta G^o = -RT \ln K_c \quad (7)$$

Ci = initial pyridine concentration (96 mg/L)
Ce = equilibrium pyridine concentration (mg/L)
Kc = thermodynamic equilibrium constant
T = absolute temperature (K)
ΔG° =standard Gibbs free energy change (kJ/mol)
ΔH° =standard enthalpy change (kJ/mol)
ΔS° =standard entropy change (J/mol·K)
R = universal gas constant (8.314 J/mol·K)

3. Results and Discussion

3.1. Changing the Designing Factors within the Studied Ranges

3.1.1. Acidic function (pH):

Fig. 2 shows the results obtained from changing the pH factor, within a range of 1-9, on the treating efficiency (%E) of

contaminated solutions by pyridine base using virgin tangerine peels powder as a low-cost, non-valuable adsorbent, at a constant contact time of 180 minutes, a tangerine peels dosage of 1 g, an agitation speed of 250 rpm, a temperature of 25 °C, and an pyridine base initial concentration of 1 ppm. Fig. 2 shows that the obtained data takes the form of a bell curve, gradually rising from a pH of 1 to a peak at a pH of 6, then decreasing dramatically to a minimum value at a pH of 9. Based on these results, the performance of the tangerine peels can be divided into three stages, the first of which is the increase in the removal efficiency (%E) in the acidic range 1-5. This is attributed to the presence of a dominant adsorption mechanism that depends almost entirely on the electrostatic charges of the tangerine peels and the chemical conditioning of the pyridine base. At very low pH values, ranging between pH=1–3, the acidity of the contaminated solution is at its highest, and in return, the removal efficiency (%E) is low ranging between 3.27–10.5%, respectively, due to the protonation (positive charge) of the functional groups on the surface of the tangerine peels such as –OH and –COOH, which causes repulsion with molecules of pyridine base [26]. On the other hand, the repulsive forces with the hydronium ions (H_3O^+) at the adsorption sites are at their peak, which explains the clear decrease in (%E). The efficiency of the tangerine peels continues to improve with increasing acidity until it reaches its peak at a pH of approximately 6, at which point the performance reaches the second stage. Upon reaching the near-neutral zone, pH=4-6, the positive charges on the surface of the adsorbent material begin to gradually decrease, the surface functional groups begin to partially deproteinize, the density of active sites increases, and the pyridine base reaches a state of partial ionization, which enhances the electrostatic attraction and hydrogen bonding forces, or van der Waals forces [27]. As a result, the repulsion decreases, and the molecules of the target material are able to bind to the functional groups at the functionally active sites, thus increasing the treating efficiency and reaching its maximum value of 23% at pH = 6, which represents an optimal equilibrium between the surface charge of the tangerine peels, adsorption capacity, and adsorption stability. After this peak performance, the increasing pH value is accompanied by a clear and continuous decrease in treating efficiency until it reaches the lowest performance level of the adsorbent. The increase in alkalinity from pH=7 to pH=9 leads to an increase in the concentration of hydroxide ions, which may compete with target molecules for adsorption sites, generating electrostatic repulsion with them. Furthermore, the weak bonds formed at intermediate pH can break down, leading to decreased treating efficiency (%E) due to the return of adsorbed molecules to the aqueous solution. On the other hand, the solubility of pyridine base is minimal in the basic range because it remains in its non-ionized (neutral) form, thus reducing adsorption potential [21]. Accordingly, the overall behavior indicates that the treatment efficiency (%E) is governed by a dual effect of pH, which includes control of surface charge, the mechanism of interaction between the adsorbent and the adsorbed material, and ion competition in the solution, with an optimal pH value of 6 achieving the highest adsorption efficiency of 23% under the studied conditions.

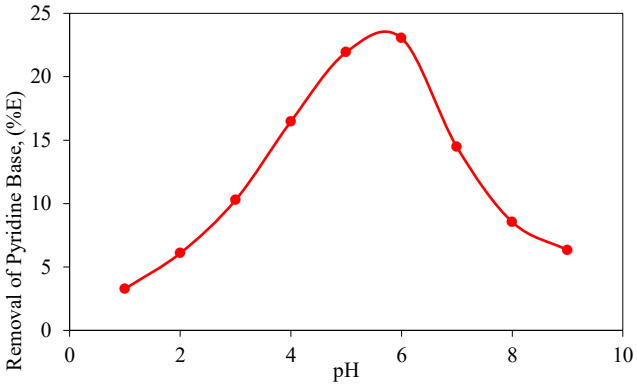

Figure 2. Influence of pH on the removal of pyridine using tangerine peels.

3.1.2. Agitation speed

Fig. 3 shows the results obtained from changing the agitation speed factor, within a range of 100-500 rpm, on the treating efficiency (%E) of contaminated solutions by pyridine base using virgin tangerine peels powder as a low-cost, non-valuable adsorbent, at a constant contact time of 180 minutes, a tangerine peels dosage of 1 g, pH of contaminated solution of 6, a temperature of 25 °C, and a pyridine base initial concentration of 1 ppm. In general, the data obtained show that the agitation speed is directly related to the treating efficiency (%E), continuing until a certain point is reached, after which the performance of the adsorbent remains constant despite increased agitation. At low agitation speeds ranging from 100 to 200 rpm, the treating efficiency (%E) values are low, between 5 and 13.6%, respectively, as the movement of pyridine molecules is limited. Furthermore, the momentum generated at these speeds is insufficient to break down the boundary film layer formed on the outer surface of the tangerine peels, thus hindering the delivery of target molecules to the active sites. Consequently, the contaminated molecules remain dispersed in the solution, keeping treatment efficiency at its minimum value. Increasing the agitation speed from 250 to 300 rpm leads to improved mass transfer in the solution due to improved hydrodynamic conditions within the aqueous medium and an increase in generated momentum, which leads to an increase in the breakdown of the boundary film layer formed on the surface of the tangerine peels [28]. This improvement will enhance the access of pyridine molecules to the active sites and lead to an increase in the capturing ability by the active functional groups, thus reducing their concentration in the solution and significantly increasing the treating efficiency (%E) from 23% to 31.6%.

It is also noticeable from Fig. 3 that increasing the agitation speed to 350 and then to 400 rpm will increase the treating efficiency (%E) from 37.7% to 43%, respectively, indicating that the mass transfer efficiency increases and the boundary film layer continues to break down, allowing for the utilization of a greater number of active sites on the surface of the tangerine peels, but at a slower rate than in the previous speed range. However, increasing the agitation speed above 400 rpm does not further increase the treating efficiency (%E), which remains constant at 43%. This is attributed to the fact that the system has actually reached a state of kinetic equilibrium or

saturation, where the rate of transport of molecules to the adsorbent surface has become equal to the rate of filling of the available active sites, or all the easily accessible surface sites have become saturated, and the controlled step is very slow internal diffusion that is not affected by external disturbance [21]. Very high speeds can also lead to disturbance in the adsorption layer or to partial desorption of the adsorbed pyridine molecules due to shear forces, preventing further improvement in the treating efficiency (%E). Thus, the overall behavior of the system reflects a balance between improved mass transfer at medium speeds and the system reaching the limits of dynamic adsorption at high speeds, which logically explains the stability of the treating efficiency (%E) despite the continued increase in agitation speed [29]. Therefore, the agitation speed that leads to the highest treating efficiency (%E) under the aforementioned operating conditions is 400 rpm.

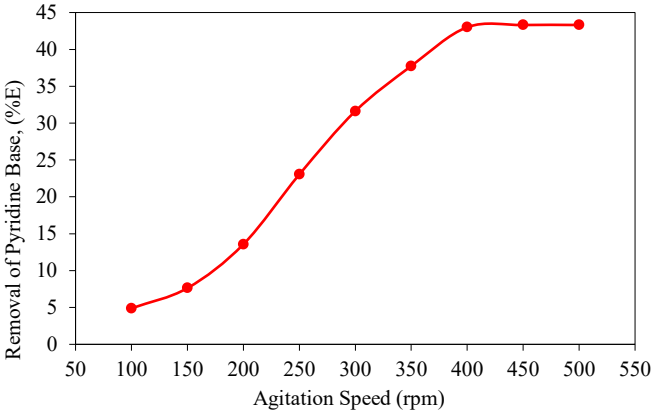

Figure 3. Influence of agitation speed on the removal of pyridine using tangerine peels.

3.1.3. Initial concentration

"It should be noted that the lower removal efficiencies (19–24%) observed at 96 mg/L were obtained using a lower adsorbent dosage (1 g), whereas the maximum removal efficiency of 83.6% was achieved only under optimized operating conditions using 5.8 g of adsorbent."

Fig. 4 shows the results obtained from changing the initial concentration of target material factor, within a range of 1-100 ppm, on the treating efficiency (%E) of contaminated solutions by pyridine base using virgin tangerine peels powder as a low-cost, non-valuable adsorbent, at a constant contact time of 180 minutes, a tangerine peels dosage of 1 g, pH of contaminated solution of 6, a temperature of 25 °C, and an agitation speed of 400 rpm. Fig. 4 shows an inverse relationship between the two variables, where increasing the initial concentration of pyridine leads to a decrease in the treating efficiency (%E), and conversely, the adsorbed concentration gradually increases until the highest adsorbed concentration is reached, which is achieved at the highest initial concentration and the lowest treating efficiency (%E). At very low concentrations (C_i = 1-10 ppm) of pyridine base, the treating efficiency (%E) is high, ranging between 38–43%. This is due to the abundance of vacant and unsaturated active sites on the surface of the tangerine peels compared to the number of pyridine molecules, allowing for the efficient and easy adsorption of a high ratio of the pollutant relative to its total quantity. Therefore, the treating efficiency (%E) records high values compared to the higher initial concentrations, although the concentration of the actually adsorbed material (C_ads) remains limited, as the adsorbed concentration C_ads does not exceed 1% of the maximum treating efficiency (%E) [30]. With increasing initial concentration (C_i=15-60 ppm), the mass motive force and the migration of the material from the liquid phase to the solid surface increase, gradually reducing the treating efficiency (%E) from 36.4% to 26%, respectively, due to the decreasing ratio of vacant sites to the increasing number of pyridine molecules, creating noticeable competition for those sites. In contrast, C_ads continues to increase from 5.5 to 15.6 ppm, almost linearly in the early stages and then with a lesser tendency at high concentrations as a result of the surface approaching saturation, because the driving force of high concentration pushes more molecules to fill the available sites, even those with weaker binding energy [31]. At very high concentrations (C_i=70-96 ppm), the treating efficiency (%E) drops dramatically from 24-19%, respectively, while C_ads remains relatively stable, increasing very slowly until it approaches a plateau at 96 ppm, which is approximately 100% of the treating efficiency (%E). It should be noted that the lower removal efficiencies (19–24%) observed at 96 mg/L were obtained using a lower adsorbent dosage (1 g), whereas the maximum removal efficiency of 83.6% was achieved only under optimized operating conditions using 5.8 g of adsorbent. This confirms that the active sites available to the tangerine peels under these conditions have been completely saturated and are no longer able to receive any additional molecules of the target adsorbed molecules. During passage of the initial concentration of 96 ppm, the %E gradually declined, but as the initial concentration increased further, %E could no longer decrease and the adsorbed concentration C_ads was relatively constant as C_ads = 19 ppm, which means that further increase in the initial concentration does not contribute to the system's improvement; thus, it is desirable that the system moved from surface control step to capacity control step. This dual behavior illustrates that the adsorbent medium is optimal at high concentrations with respect to its capacity, and at low concentrations with respect to its treating efficiency (% E). Such behaviors are indicative of typical physical and chemical adsorption systems and are a manifestation of the interplay between the type of the surface, number density of reactive sites, and the transport and diffusion mechanisms [26].

3.1.4. Adsorbent dosage

Fig. 5 shows the results obtained from changing the adsorption dosage factor, within a range of 0.5-6 g, on the treating efficiency (%E) of contaminated solutions by pyridine base using virgin tangerine peels powder as a low-cost, non-valuable adsorbent, at a constant contact time of 180 minutes, a pyridine base initial concentration of 96 ppm, pH of contaminated solution of 6, a temperature of 25 °C, and an agitation speed of 400 rpm. Observing the results reveals that the adsorbent dosage exhibits a dual behavior: increasing it from 0.5 to 6 grams leads to a significant increase in the treating efficiency (%E) from 10% to 83.6%, respectively, while simultaneously decreasing the adsorption capacity (q) by 31%. At very low doses ranging from 0.5g to 2 g, the values of treating efficiency

(%E) are modest, ranging between 10–38.5%, respectively, due to insufficient total active sites to handle the total number of organic molecules in a constant volume of solution, resulting from the limited available surface area. However, the value of adsorption capacity (q) is relatively high (1.9–1.5 mg/g) because each gram of adsorbent functions at maximum efficiency, with optimal access to the adsorbed material and no competition between the target pyridine molecules. As the adsorption dosages move into the medium range (2.5-4.5 g), the treating efficiency (%E) continues to increase from 47.2% to 73.5%, respectively, in a quasi-linear manner as a result of the provision of additional sites and an increase in surface area, while the adsorption capacity (q) continues to decrease (from 1.8 to 1.56 mg/g) due to the partial aggregation of the tangerine peels, where they block each other and reduce the exposure of the effective surface per unit mass. Also, the residual concentration of the substance in the solution decreases rapidly, which reduces the driving force of adsorption on each subsequent gram. Increasing the adsorption dose provides a greater number of effective sites and total surface area available for capturing the target organic molecules, which enhances the treating efficiency (%E) of the contaminated solution, and raises %E from very low values at small masses to a semi-steady state at high masses [32]. In contrast, the continuous decrease in adsorption capacity (q) with increasing dosage is explained by the distribution of a constant amount of the adsorbed material over a larger mass of the solid medium, which leads to a decrease in specific load per gram, in addition to the possibility of overlapping or clumping of particles of the adsorption medium at high doses, which reduces the effectiveness of some surface sites and limits the full utilization of the actually available space [29]. At high doses (5-6 g), the improvement in treating efficiency (%E) slows down considerably and then stabilizes at a maximum value of 83.6%, while the adsorption capacity (q) decreases to its minimum value (1.34 mg/g), indicating that the system has reached the level of saturation possible under the current experimental conditions, and that additional doses have become insignificantly effective and barely contribute to the adsorption of the target molecules, since most of the pyridine molecules have already been removed and the remaining vacant sites cannot be efficiently exploited [31]. The stability of the treating efficiency (%E) while the adsorption capacity (q) continues to decrease indicates that the balance between achieving high treating efficiency (%E) and efficient use of the adsorbent is achieved at an approximate optimal dose of 5.8 g, where (%E) is close to the maximum and the adsorption capacity (q) is still at an acceptable level.

3.1.5. Contact time

Fig. 6 shows the results obtained from changing the contact time factor, within a range of 10-180 minutes, on the treating efficiency (%E) of contaminated solutions by pyridine base using virgin tangerine peels powder as a low-cost, non-valuable adsorbent, at a constant tangerine peels dosage of 5.8 g, a pyridine base initial concentration of 96 ppm, pH of contaminated solution of 6, a temperature of 25 °C, and an agitation speed of 400 rpm. The experimental results show that the contact time is directly related to the treating efficiency (%E); a longer contact time leads to a higher treating efficiency (%E), and vice versa. This result can be attributed to the classical kinetic behavior of the adsorption process, and three main time stages related to mass transfer and saturation mechanisms can be distinguished. In the initial stage, which lasts between 10 and 45 minutes, the increase in the treating efficiency (%E) is relatively slow, from 7% to 29.4%, respectively, because it is mainly governed by slow external diffusion and a low number of adsorbed molecules due to the limited initial binding [30].

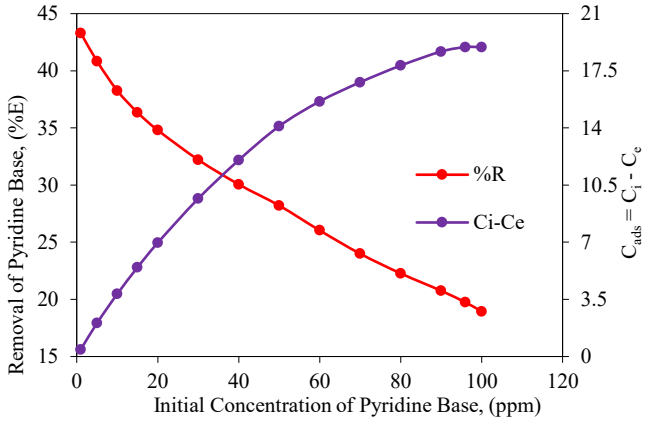

Figure 4. Influence of initial concentration on the removal of pyridine using tangerine peels.

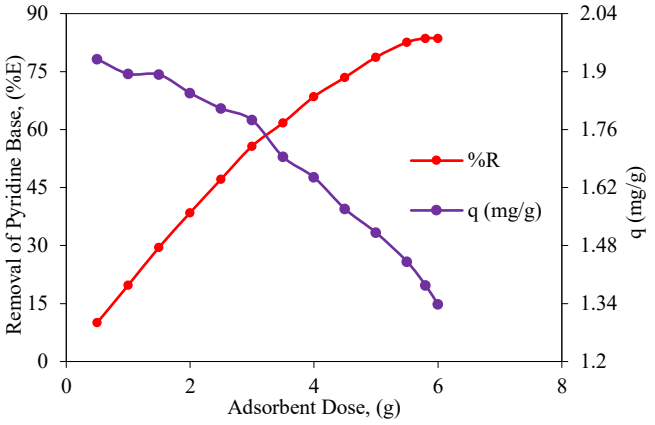

Figure 5. Influence of adsorbent dosage on the removal of pyridine using tangerine peels.

This is because adsorption initially occurs at the most readily available active sites on the outer surface of the tangerine peel particles, and the initial diffusion of organic pyridine base molecules across the static boundary layer surrounding each particle constitutes an initial resistance that takes time to overcome [21]. Subsequently, the results show that increasing the contact time leads to a gradual improvement in the treating efficiency (%E) due to the increased contact time between the adsorbent medium and the contaminating pyridine molecules. The process enters a phase of sharp acceleration in the time period between 60 and 120 minutes, during which the treating efficiency (%E) increases rapidly from 38.1% to 69%. This is attributable to the certainty of abundant free surface areas and the dominating diffusion processes in pores and the mechanism of physical or chemical bonds, which depend on the type of the adsorbent medium. Compared to the time spans, the surface

area of these pores provides more adsorption sites. Additionally, the concentration gradient (concentration in the solution versus concentration on the surface) is still large, so the driving force for the molecules to move is still strong [29]. In the last phase of time, 150 to 180 minutes, the treatment is in a stabilization or saturation phase, with little change in treating efficiency (%E), with DBPS at 150 min at 83.6%, suggesting the dynamic equilibrium had been established. In this stage, the adsorption and detachment rates of pyridine molecules from the surface of tangerine peels are approximately equal. In addition, the remaining molecules may not be able to access deeper pore sites because of a diffusion barrier or molecular repulsion, and further uptake therefore results in the saturation of all active sites in the surface or bulk. This behavior could also be related to the reduction in mass transport driving force due to the decreasing organic matter concentration in the solution over time, and likely the saturation of the adsorption capacity of the medium [26]. These explanations corroborate the fact that progressively increasing the treatment time past the equilibrium point of 150 min does not allow for enhancing the treatment efficacy (%E), rather reflects the loss of time and energy with no evident benefit at the end.

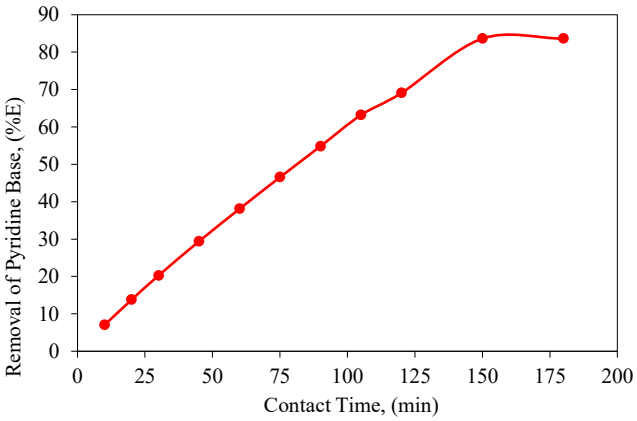

Figure 6. Influence of contact time on the removal of pyridine using tangerine peels.

3.1.6. Temperature

Fig. 7 shows the Van't Hoff plot exhibited a good linear relationship with a correlation coefficient of R=0.9817, indicating the suitability of the thermodynamic model for describing pyridine adsorption onto tangerine peels. The calculated enthalpy change ($\Delta H^\circ = -156.27$ kJ/mol) confirmed that the adsorption process was exothermic in nature. The negative entropy value ($\Delta S^\circ = -511.15$ J/mol·K) suggested a decrease in randomness at the solid–liquid interface during adsorption. Furthermore, the negative Gibbs free energy values at lower temperatures demonstrated the spontaneous nature of pyridine adsorption under ambient conditions. However, the gradual increase in ΔG° values with temperature indicated that higher temperatures reduced adsorption efficiency, making the adsorption process less favorable at elevated temperatures. The increased temperature may also induce slight changes in the pore structure or surface charges of the adsorbent itself, which can decrease their adsorption efficiency [30].

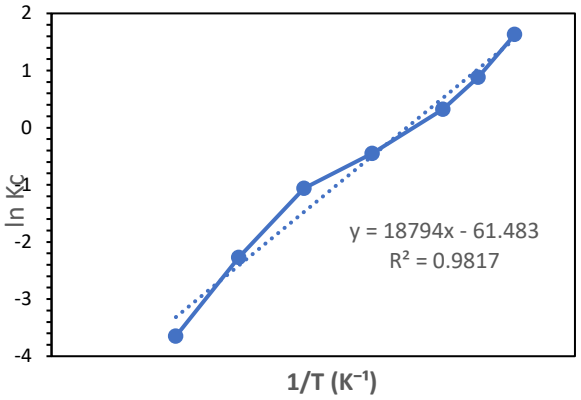

Figure 7. Van't Hoff plot for pyridine adsorption onto tangerine peels.

3.1.7. Adsorption isotherm models

Adsorption isotherm models were applied to evaluate the interaction between pyridine molecules and the surface of tangerine peels and to estimate the biosorbent's adsorption capacity. Adsorption isotherm models are commonly used to describe the interaction between adsorbate molecules and the surface of adsorbents at equilibrium conditions. Table 1: These models provide important information regarding adsorption mechanisms, surface characteristics, and adsorption capacity. In the present study, the Langmuir and Freundlich isotherm models were applied to evaluate the equilibrium adsorption behavior of pyridine onto tangerine peels and to determine the biosorbent's suitability for wastewater treatment applications.

Table 1. Comparison of adsorption isotherm models for pyridine adsorption onto tangerine peels.

Model	Linear equation	Parameters	Value	R^2	Main interpretation
Langmuir	y = 3.8083x + 0.4773	q_{max} (mg/g)	2.095	0.9919	Best-fitting model indicating monolayer adsorption on a homogeneous surface
		K_L (L/mg)	0.125		
Freundlich	y = 0.1905x − 0.1676	K_F	0.680	0.9745	Indicates favorable adsorption on a heterogeneous surface
		n	5.249		Favorable adsorption process

The obtained isotherm results demonstrated that the Langmuir model provided a better fit for the experimental data compared with the Freundlich model, as indicated by the higher correlation coefficient (R^2=0.9919). Fig. 8 and 9. This suggests that pyridine adsorption onto tangerine peels predominantly occurred as monolayer adsorption on relatively homogeneous adsorption sites. In addition, the Freundlich constant (n=5.249) confirmed favorable adsorption behavior. Although the calculated adsorption capacity (q_{max}=2.095 mg/g) was lower than some chemically modified adsorbents reported in previous studies, the present work demonstrated that untreated tangerine peels can still achieve considerable pyridine removal efficiency under optimized operating conditions. Although the calculated adsorption capacity (q_{max}=2.095 mg/g) was lower than some chemically modified adsorbents reported in previous studies, the present study still achieved a considerable pyridine removal efficiency of 83.6% under optimized operating conditions. The relatively lower adsorption capacity may be attributed to the absence of activation or chemical modification processes. Nevertheless, the proposed biosorbent offers significant advantages including low cost, biodegradability, environmental sustainability, and agricultural waste valorization.

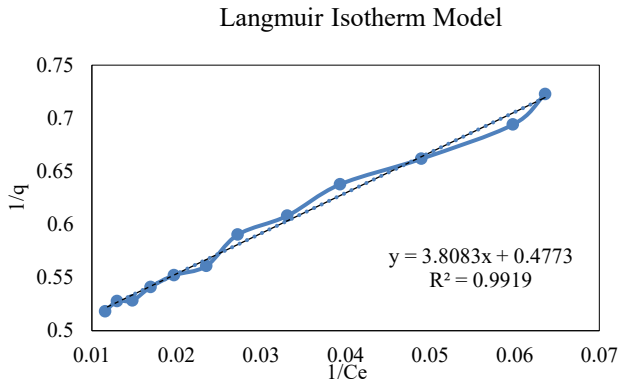

Figure 8. Langmuir isotherm model for pyridine adsorption onto tangerine peels.

3.1.8 Adsorption kinetic models

The adsorption kinetics of pyridine onto tangerine peels were evaluated using pseudo-first-order, pseudo-second-order, Elovich, and intra-particle diffusion kinetic models to better understand the adsorption mechanism and rate-controlling steps. The obtained kinetic parameters and correlation coefficients for the applied adsorption kinetic models are summarized in Table 2.

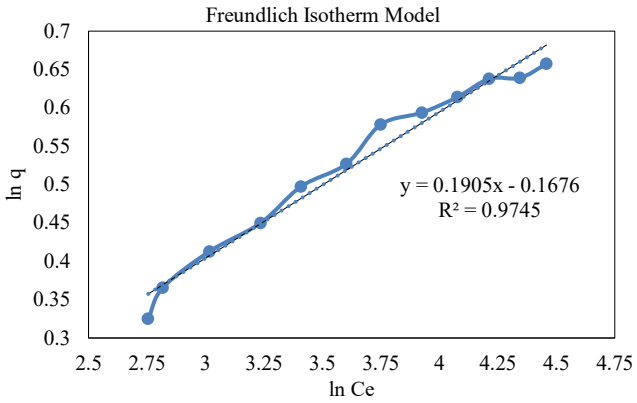

Figure 9. Freundlich isotherm model for pyridine adsorption onto tangerine peels.

The adsorption kinetic results demonstrated that the intra-particle diffusion model exhibited the highest correlation coefficient (R^2=0.9879), suggesting that diffusion within the pores of tangerine peels played a significant role during pyridine adsorption. The Elovich model also showed a relatively high fitting accuracy (R^2=0.9132), indicating heterogeneous adsorption behavior and possible surface interaction effects. In contrast, the pseudo-first-order model showed poor agreement with the experimental data (R^2=0.6197), while the pseudo-second-order model provided moderate fitting (R^2=0.8953). Figs 10-13. Overall, the obtained kinetic results suggested that pyridine adsorption onto tangerine peels was influenced mainly by intra-particle diffusion accompanied by heterogeneous surface adsorption mechanisms. The obtained thermodynamic, kinetic, and isotherm results provided important insight into the adsorption mechanism of pyridine onto tangerine peels. The Langmuir isotherm model showed the best fit (R^2=0.9919), indicating monolayer adsorption on relatively homogeneous adsorption sites. In addition, the intra-particle diffusion model exhibited the highest correlation coefficient among the applied kinetic models (R^2=0.9879), suggesting that pore diffusion played a major role in controlling the adsorption process. Furthermore, the relatively high enthalpy change (ΔH°=−156.27 kJ/mol) together with the fitting behavior of the Elovich and pseudo-second-order kinetic models suggested the contribution of chemical interactions during adsorption. Overall, the obtained results indicated that pyridine adsorption onto tangerine peels involved combined diffusion and surface interaction mechanisms.

Table 2. Comparison of kinetic models for pyridine adsorption onto tangerine peels.

Model	Linear equation	R^2	Main interpretation
Pseudo-first-order	y = −0.0365x + 1.5114	0.6197	Poor fitting indicating weak applicability of the model for pyridine adsorption kinetics
Pseudo-second-order	y = 0.2142x + 81.998	0.8953	Moderate fitting suggesting partial contribution of surface adsorption interactions
Elovich	y = 0.4635x − 1.1433	0.9132	Indicates heterogeneous adsorption behavior and surface interaction effects

Model	Linear equation	R^2	Main interpretation
Intra-particle diffusion	y = 0.1411x − 0.4124	0.9879	Best-fitting model indicating that intra-particle diffusion significantly influenced the adsorption process

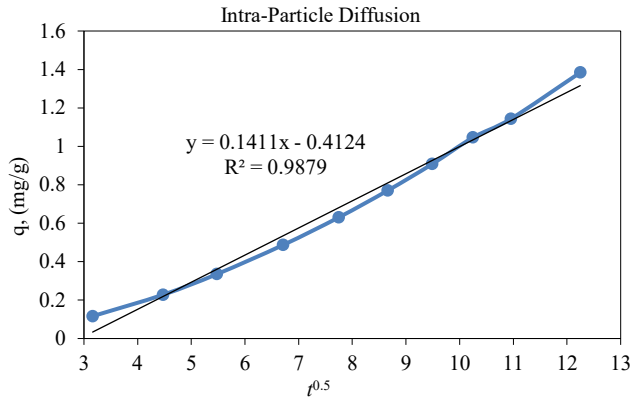

Figure 10. Intra-particle diffusion model for pyridine adsorption onto tangerine peels.

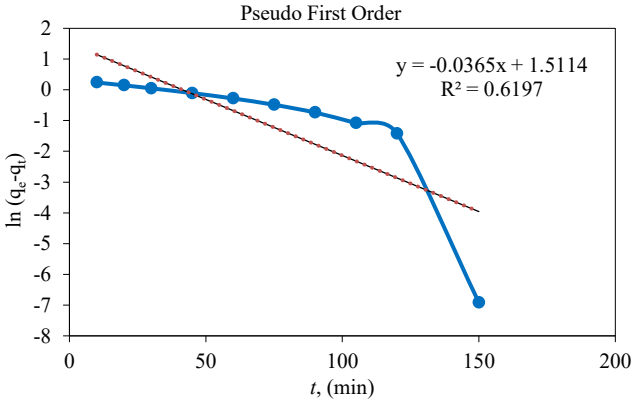

Figure 11. Pseudo-first-order kinetic model for pyridine adsorption onto tangerine peels.

3.2. Morphological Changes in the Tangerine Peels

3.2.1. Fourier transform infrared spectroscopy (FT-IR):

Fig. 14 shows the results obtained from performing Fourier transform infrared spectroscopy on tangerine peels used as an adsorption medium for recovering organic pyridine base molecules from contaminated aqueous solutions. The blue curve shows the FTIR analysis of virgin tangerine peels, while the red curve shows the FTIR analysis of tangerine peels after treatment with pyridine-contaminated solutions. FTIR analysis shows that the adsorption process led to clear changes in the distribution and disappearance of some spectral peaks with the appearance of new peaks, indicating the occurrence of physical and chemical interactions between the adsorption medium and the target material molecules. The FTIR spectrum of virgin tangerine peels shows a set of distinctive peaks reflecting the chemical nature of the surface, where the broad peak extending between wavelengths of approximately 3600–3200 cm-1 is attributed to tension vibrations of hydroxyl (O–H) groups associated with surface water or alcohol and phenolic groups, while the relatively weak peaks near 2920–2850 cm-1 indicate tension vibrations of aliphatic C–H groups.

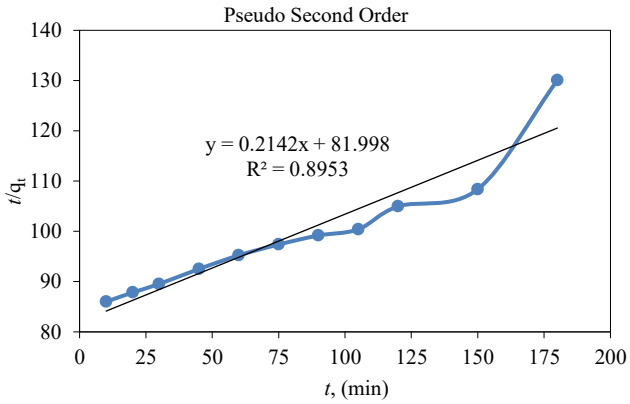

Figure 12. Pseudo-second-order kinetic model for pyridine adsorption onto tangerine peels.

The pronounced peak around 1700–1600 cm-1 is attributed to tensile vibrations of the C=O bond of a carboxyl group or to flexural vibrations of the water molecule. The peaks located between 1400–1500 cm-1 are attributed to aromatic C=C vibrations or to O–H and C–H bonds. The imprinting region between 1000–1300 cm-1 is attributed to tensile vibrations of C–O and C–O–C groups, depending on the organic composition of the tangerine peels, which consist of a high percentage of cellulose and lignin. Meanwhile, the multiple sharp peaks below 1000 cm-1 are associated with structural and compositional vibrations outside the spatial plane of various functional groups on the surface. After adsorption, a general decrease in sample transparency is observed due to a drop in %T across most wavenumber ranges, indicating increased photon absorption due to the formation of new bonds or the coverage of a large number of active sites.

Changes in the scales of the tangerine peels after treatment with pyridine-contaminated solutions include the disappearance or decrease in the intensity of most of the peaks, the widening or displacement of some peaks, and the appearance of other peaks. In the range between 3600-3200 cm-1, the disappearance and decrease of peaks associated with tensile vibrations of hydroxyl and amine O-H bonds are observed, indicating the involvement of O-H or N-H groups in the pyridine adsorption process through hydrogen bond formation or chemical reactions.

Notable changes can also be indicated by the shift and modification in the 2800-2400 cm-1 range attributed to the C-H organic bond vibrations, indicating their direct interaction with contaminating pyridine molecules via physical attractive forces or weak surface complexes. While the 1600-1200 cm-1 range shows the emergence of new peaks in addition to the strengthening of existing peaks, which are attributed to single and double oxygen bonds C-O and C=O and nitrogen bonds C-N, this confirms the formation of new bonds and a modification

in the chemical environment of the original functional groups. The observed changes in this range likely reflect (π-π) bonds between the aromatic rings of the organic pyridine base and the surface of the adsorbed tangerine peels due to a redistribution of surface electrons. Coating the active sites on the tangerine peel surface with a layer of organic pyridine molecules resulted in a marked decrease in peak intensity within the 800–1200 cm-1 range, confirming the active participation of functional groups within this range in adsorption, thus reducing the penetration of infrared radiation into the pores in this wavelength range. Finally, the spectral changes also extended to the lower wavelength range, ≤ 800 cm-1, where most peaks disappeared or were significantly reduced. This suggests covalent interactions and structural changes at the adsorption surface, and further confirms the active contribution of functional groups in this range to the highly efficient retention of organic pyridine molecules. These spectral changes, characterized by shifts and changes in the original peaks, as well as the disappearance and emergence of new peaks, support the hypothesis that the adsorption is chemical in nature, with some weak physical mechanisms also contributing [26].

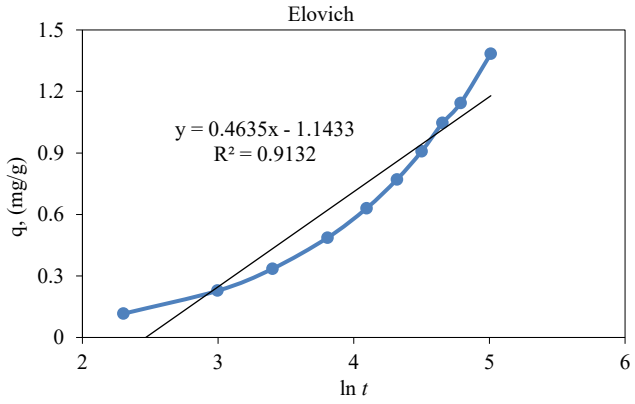

Figure 13. Elovich kinetic model for pyridine adsorption onto tangerine peels.

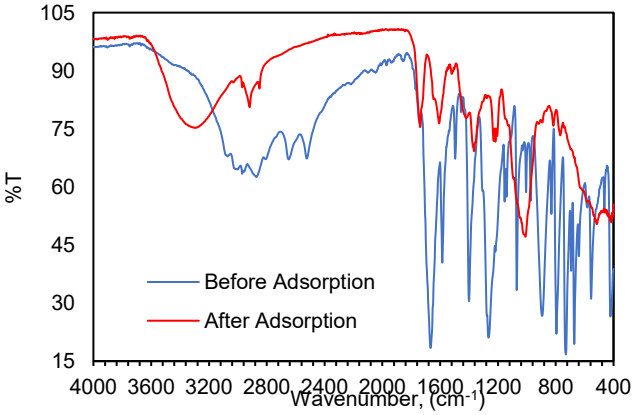

Figure 14. FT-IR of tangerine peels, before and after, used as an adsorbent for pyridine.

3.2.2. Specific surface area (SBET):

Fig. 15 illustrates the results obtained from surface area analysis using the BET technique on tangerine peels used as an adsorption medium for recovering organic pyridine base molecules from contaminated aqueous solutions. The blue curve shows that the surface area of virgin tangerine peels is 15.59 m2/g, while the red curve shows that the surface area of tangerine peels after treatment with pyridine-contaminated solutions is 3.25 m²/g. This sharp decrease in surface area indicates profound structural changes in the morphology of the adsorbent medium, providing direct and strong evidence of effective adsorption of the target material onto the surface. This significant decrease in surface area indicates the occupation of primarily active sites and the blockage of pores or extensive coverage of the internal and external surfaces of virgin tangerine peels. This change reflects the occupation and accumulation of micro- and macro-sized pores by pyridine molecules, resulting in the covering of a large number of active sites that were available before adsorption. This, in turn, reduces the surface area accessible to the nitrogen gas used in surface area analysis. Another almost certain possibility is that physical changes have occurred, such as swelling of the surface structure of the tangerine peels as a result of treatment with the pyridine-contaminated solution, leading to pore constriction, or that strong chemical reactions have taken place between the active sites on the surface and the target molecules, leading to the deposition of adsorbed molecules and the formation of a thick layer on the outer and inner surfaces, permanently obscuring large areas and confirming the hypothesis of chemical adsorption. This decrease in surface area may also be attributed to the formation of a continuous or semi-continuous adsorbent layer on the outer and inner surfaces of the adsorbent medium, acting as a physical barrier that reduces surface roughness and limits interaction with the surrounding environment. It is possible that the organic pyridine base molecules contributed to the partial irreversible blockage of the micropores, which explains the significant decrease in surface area value after adsorption compared to the initial value of the virgin tangerine peels. In general, this sharp decrease in surface area after adsorption reflects the success of the removal process and confirms that adsorption was not limited to the outer surface only, but included the internal pores and active sites with joint mechanisms that are predominantly chemical in nature and supported by weak physical surface interactions, which led to a significant reduction in the pore structure available for measurement [33].

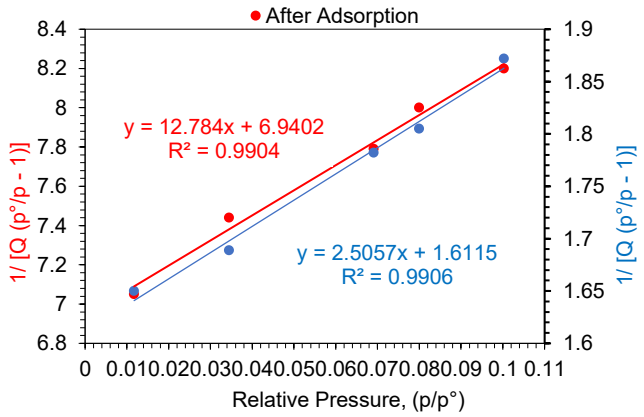

Figure 15. BET surface area of tangerine peels, before and after, used as an adsorbent of pyridine.

3.2.3. Field emission scanning electron microscopy (FESEM)

Fig. 16 shows the results obtained from scanning electron microscopy (FESEM) examination of tangerine peels used as an adsorption medium for recovering organic pyridine base molecules from contaminated aqueous solutions. Fig. 16a shows the FESEM image of virgin tangerine peels, while Fig. 16b shows the FESEM image of tangerine peels after treatment with pyridine-contaminated solutions. Before adsorption, the FESEM image, shown in Figure 16a, reveals that the virgin tangerine peels possess an irregular, lamellar, and undulating surface with numerous cracks, cavities, and interstitial spaces of varying sizes. This suggests an irregular skeleton, a wide pore size distribution, and rich species with potential active sites for target molecule trapping. In addition, the accumulation of surface roughness/rugosity and sharp edges/overlap that arise from morphological heterogeneity and surface defects may provide numerous open pores and transport pathways for promoting adsorption processes. The morphology of the tangerine peels after treatment with the solution contaminated with an organic base (pyridine) was representative of this change, as shown in Fig. 16b. The resulting observable outcome is a drop in the relative roughness shown in Fig. 16b, also with fewer or completely closed cracks and open cavities leading to smoother and tighter zones. Besides being able to see a specific size of small particles or lumps spread on the surface, as well as between lamellar surfaces (this is explained by deposition of adsorbed organic pyridine base inside pores and on active sites) or formation of an adsorbed layer that completely covers the surface, which can either be

partial depositional. Furthermore, the filling of intercellular spaces and the blockage of some pore channels indicate penetration of the target organic base molecules into the structure of the adsorbent medium, rather than mere external surface adsorption. On the other hand, changes in sheet thickness or proximity reflect structural rearrangements resulting from physical forces such as van der Waals forces, hydrogen bonds, or electrostatic interactions between the surface of the tangerine peels and pyridine molecules, thus confirming previous FTIR analysis interpretations. The images do not show evidence of fragmentation or sharp structural collapse, indicating that the adsorption process did not damage the original structure of the adsorbent medium but was limited to modifying its surface morphology as a result of the occupation of active sites. Overall, the clear transition from a rough, porous surface before adsorption to a fuller, smoother surface after adsorption is direct evidence of the success of the adsorption process, and confirms that the removal of the target organic molecules occurred through a combination of mechanisms including pore filling, surface coating with an adsorbent layer, and the formation of organic aggregates bound to the adsorbent medium, with the predominance of chemisorption supported by weak physical surface interactions [24].

4. Comparison with Previous Studies

Table 3 presents a comparison between the present study and previously published studies regarding pyridine adsorption using different adsorbents reported in the literature.

Table 3 compares the adsorption performance of tangerine peels with previously reported adsorbents for pyridine removal from aqueous solutions. Although some conventional adsorbents such as activated carbon exhibited higher removal efficiencies, the present study demonstrated that untreated tangerine peels can achieve considerable pyridine removal efficiency (83.6%) under optimized conditions. The obtained results highlight the potential of tangerine peels as an inexpensive, environmentally friendly, and sustainable biosorbent for wastewater treatment applications. In addition, the utilization of agricultural waste materials contributes to waste minimization and supports sustainable environmental management practices.

Table 3. Comparison of pyridine adsorption performance using different adsorbents reported in previous studies.

Adsorbent	Pollutant	Removal Efficiency (%)	Adsorption Capacity (qmax, mg/g)	Remarks	Reference
Activated carbon cloth	Pyridine	~90%	70	High adsorption due to π–π interactions	García-Hernández et al., 2022 [28]
Coke powder	Pyridine	76%	31.8	Low-cost industrial adsorbent	Gao et al., 2019 [21]
Activated carbon from agricultural waste	Pyridine	84–96%	45	Effective adsorption at low concentrations	Mohan et al., 2004 [34]
Rice husk ash (RHA)	Pyridine	79.5%	28.4	Agricultural waste adsorbent	Latane, et al., 2008 [35]
nZVI/GAC composite	Pyridine	86%	52	Composite adsorbent with enhanced activity	Gosu et al., 2016 [36]
Tangerine peels (Present study)	Pyridine	83.6%	2.095	Eco-friendly and low-cost biosorbent	Present study

Although the obtained adsorption capacity (q_{max}=2.095 mg/g) was lower than some highly engineered and chemically modified adsorbents reported in the literature, the present study demonstrated that untreated tangerine peels can still provide considerable pyridine removal efficiency under optimized conditions. The relatively lower adsorption capacity may be attributed to the absence of physical or chemical activation processes, which are commonly used to enhance surface area and active adsorption sites in commercial adsorbents. Nevertheless, the use of raw tangerine peels offers important advantages including low cost, environmental sustainability, biodegradability, and waste valorization.

The relatively high adsorbent dosage needed in the current study could also be explained by the use of raw and non-activated tangerine peels, as they were not treated chemically or thermally. However, the study showed that agricultural waste products can achieve high pyridine elimination efficiency using environmentally sustainable, low-cost techniques.

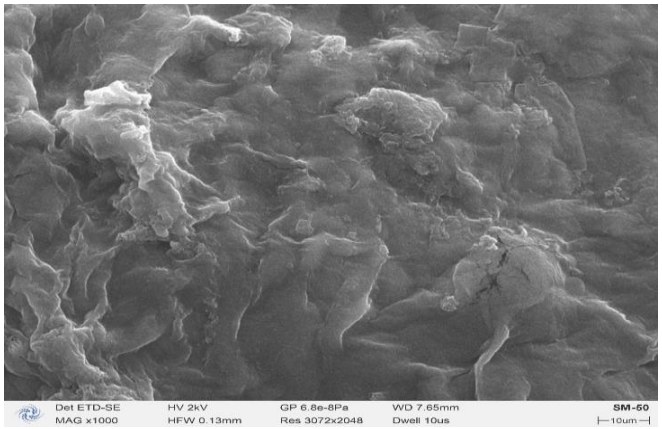

a. before adsorption.

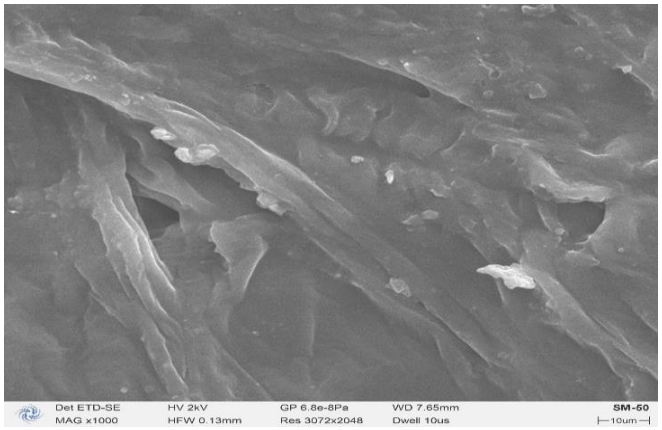

b. after adsorption.

Figure 16. FESEM image of tangerine peels

5. Conclusions

The present study demonstrated the potential applicability of untreated tangerine peels as an inexpensive and environmentally sustainable biosorbent for pyridine removal from contaminated aqueous solutions. The experimental results revealed that a 5.8 g dosage of virgin tangerine peels achieved a maximum pyridine removal efficiency of 83.6% for an initial pyridine concentration of 96 mg/L under optimized operating conditions, including pH 6, agitation speed of 400 rpm, and contact time of 150 min at room temperature. The adsorption efficiency was strongly influenced by operational parameters such as pH, adsorbent dosage, contact time, agitation speed, temperature, and initial pyridine concentration. Surface characterization analyses confirmed the occurrence of adsorption on the tangerine peel surface. FESEM images showed noticeable morphological changes after adsorption, while FTIR analysis confirmed the involvement of various functional groups in the adsorption process. In addition, the surface area decreased from 16 to 3.25 m^2/g after adsorption, indicating occupation of active adsorption sites by pyridine molecules. Adsorption isotherm studies showed that the Langmuir model provided the best fit for the experimental data R^2 = 0.9919, suggesting monolayer adsorption on relatively homogeneous adsorption sites, with a maximum adsorption capacity q_{max} of 2.095 mg/g. Freundlich analysis also confirmed favorable adsorption behavior with an n value of 5.249. Kinetic studies demonstrated that the intra-particle diffusion model exhibited the highest fitting accuracy R^2= 0.9879, indicating that pore diffusion played a dominant role in controlling the adsorption process. The Elovich and pseudo-second-order models also suggested the contribution of surface adsorption interactions during pyridine uptake. Furthermore, thermodynamic analysis confirmed that the adsorption process was exothermic in nature due to the negative enthalpy change. ΔH^o = -156.27 kJ/mol. Overall, the obtained findings demonstrated that untreated tangerine peels can serve as an effective low-cost biosorbent and represent a promising agricultural waste material for sustainable wastewater treatment applications.

Acknowledgements

The authors acknowledge the faculty of Engineering, Mustansiriyah University (www.uomustansiriyah.edu.iq), for their valuable support.

Conflict of interest

The authors declare that there is no conflict of interest regarding the publication of this paper.

Author Contribution Statement

Nadia Matar Almhana and Zainab A. Naser: proposed the research concept and designed the experimental methodology.

Manar Banwan Hasan and Marwan Arkan Hussein: carried out the adsorption experiments and collected the experimental data.

Israa M. Al-Tameemi: performed the data analysis, verified the analytical methods, and supervised the research process.

Ola Tareq Al-Hussain: contributed to data interpretation and assisted in writing and revising the manuscript.

All authors discussed the results and approved the final version of the manuscript.

References

[1] Y. Yu, H. Jin, and Q. Lu, "Effect of polycyclic aromatic hydrocarbons on immunity," *Journal of Translational Autoimmunity*, vol. 5, p. 100177, 2022, doi: https://doi.org/10.1016/j.jtauto.2022.100177

[2] M. H. El-Saeid, A. G. Alghamdi, and A. J. Alzahrani, "Impact of atmospheric polycyclic aromatic hydrocarbons (PAHs) of falling dust in urban area settings: Status, chemical composition, sources and potential human health risks," *International Journal of Environmental Research and Public Health*, vol. 20, no. 2, p. 1216, 2023, doi: https://doi.org/10.3390/ijerph20021216

[3] F. L. Arens *et al.*, "Exploring organic compound preservation through long-term in situ experiments in the Atacama Desert and the relevance for Mars," *Scientific Reports*, vol. 15, no. 1, p. 29957, 2025, doi: https://doi.org/10.1038/s41598-025-16197-w

[4] M. Barathan, S. L. Ng, Y. Lokanathan, M. H. Ng, and J. X. Law, "Plant defense mechanisms against polycyclic aromatic hydrocarbon contamination: Insights into the role of extracellular vesicles," *Toxics*, vol. 12, no. 9, p. 653, 2024, doi: https://doi.org/10.3390/toxics12090653

[5] C. Duan, M. Tanaka, M. Kishida, and T. Watanabe, "Treatment of pyridine in industrial liquid waste by atmospheric DC water plasma," *Journal of Hazardous Materials*, vol. 430, p. 128381, 2022, doi: https://doi.org/10.1016/j.jhazmat.2022.128381

[6] D. M. Smith, "Compounds containing Six-membered Rings with one Nitrogen atom; Pyridine and its derivatives," in *Rodd's Chemistry of Carbon Compounds*, Elsevier, 1964, pp. 27–226. doi: https://doi.org/10.1016/b978-044453345-6.50749-5

[7] R. A. Pandey *et al.*, "Biotreatment of waste gas containing pyridine in a biofilter," *Bioresource Technology*, vol. 98, no. 12, pp. 2258–2267, 2007, doi: https://doi.org/10.1016/j.biortech.2006.05.015

[8] PubChem, "Pyridine, CID 1049." National Center for Biotechnology Information. Accessed: Aug. 21, 2026. [Online]. Available: https://pubchem.ncbi.nlm.nih.gov/compound/1049

[9] J. G. Zaller *et al.*, "Unexpected air pollutants with potential human health hazards: nitrification inhibitors, biocides, and persistent organic substances," *Science of the Total Environment*, vol. 862, p. 160643, 2023, doi: https://doi.org/10.1016/j.scitotenv.2022.160643

[10] IARC Working Group on the Evaluation of Carcinogenic Risks to Humans, "Exposure Data," in *Some Chemicals That Cause Tumours of the Urinary Tract in Rodents* (IARC Monographs on the Evaluation of Carcinogenic Risks to Humans, No. 119), Lyon, France: International Agency for Research on Cancer, 2019. [Online]. Available: https://www.ncbi.nlm.nih.gov/books/NBK546952/

[11] D. Hodges, "Discovery, research and development of axalion® active insecticide: dimpropyridaz†," *Pest Management Science*, vol. 81, no. 5, pp. 2529–2534, May 2025, doi: https://doi.org/10.1002/ps.8385

[12] A. A. Altaf, A. Shahzad, Z. Gul, N. Rasool, A. Badshah, B. Lal, and E. Khan, "A Review on the Medicinal Importance of Pyridine Derivatives," *Journal of Drug Design and Medicinal Chemistry*, vol. 1, no. 1, pp. 1–11, 2015, https://sciencepublishinggroup.com/article/10.11648/j.jddmc.20150101.11

[13] G. B. Daware and P. R. Gogate, "Intensified sonochemical degradation of 2-Picoline in combination with advanced oxidizing agents," *Ultrasonics Sonochemistry*, vol. 77, p. 105702, 2021, doi: https://doi.org/10.1016/j.ultsonch.2021.105702

[14] J. Ping *et al.*, "Effect of reactive oxygen species (ROS) produced by pyridine and quinoline on NH4+-N removal under phenol stress: The shift of nitrification pathway and its potential mechanisms," *Water Research*, vol. 267, p. 122478, 2024, doi: https://doi.org/10.1016/j.watres.2024.122478

[15] E. A. J. Giraud and A. T. Ford, "The effects of pyridine hydrochloride on sublethal behavioural endpoints in the common shore crab, Carcinus maenas," *Ecotoxicology*, vol. 35, no. 1, p. 4, Jan. 2026, doi: https://doi.org/10.1007/s10646-025-02993-7

[16] IARC Working Group on the Evaluation of Carcinogenic Risks to Humans, "Pyridine," in *Some Chemicals That Cause Tumours of the Urinary Tract in Rodents* (IARC Monographs on the Evaluation of Carcinogenic Risks to Humans, No. 119), Lyon, France: International Agency for Research on Cancer, 2019. [Online]. Available: https://www.ncbi.nlm.nih.gov/books/NBK546905/

[17] Agency for Toxic Substances and Disease Registry (ATSDR), "Toxicological Profile for Pyridine." Atlanta, GA: U.S. Department of Health and Human Services, Public Health Service, 1992. Accessed: Aug. 21, 2026. [Online]. Available: https://www.atsdr.cdc.gov/toxprofiles/tp52.pdf

[18] "Pyridine | Public Health Statement | ATSDR." Accessed: Mar. 15, 2026. [Online]. Available: https://wwwn.cdc.gov/TSP/PHS/PHS.aspx?phsid=533&toxid=96

[19] Y. Wu *et al.*, "Adsorptive Removal of Pyridine from Aqueous Solution Using Natural Shale," *OJOGas*, vol. 06, no. 02, pp. 36–49, 2021, doi: https://doi.org/10.4236/ojogas.2021.62004

[20] M. Namvar-Mahboub, F. Ahsani, and S. Ansari, "Preparation and Characterization of Nanosized Pomegranate Peel-Based Activated Carbon for Application in Pyridine Removal from Aqueous Solution," *Theor Found Chem Eng*, vol. 54, no. 5, pp. 940–948, Sep. 2020, doi: https://doi.org/10.1134/s0040579520050371

[21] Q. Gao, L. Wang, Z. Li, Y. Xie, Q. He, and Y. Wang, "Adsorptive removal of pyridine in simulation wastewater using coke powder," *Processes*, vol. 7, no. 7, p. 459, 2019, doi: https://doi.org/10.3390/pr7070459

[22] S. Liu *et al.*, "Advanced reduction process to achieve efficient degradation of pyridine," *Chemosphere*, vol. 287, p. 132240, 2022, doi: https://doi.org/10.1016/j.chemosphere.2021.132240

[23] D. Li *et al.*, "Electrochemical degradation of pyridine by Ti/SnO2–Sb tubular porous electrode," *Chemosphere*, vol. 149, pp. 49–56, 2016, doi: https://doi.org/10.1016/j.chemosphere.2016.01.078

[24] A. S. El-Shafie, E. Rahman, Y. GadelHak, R. Mahmoud, and M. El-Azazy, "Techno-economic assessment of waste mandarin biochar as a green adsorbent for binary dye wastewater effluents of methylene blue and basic fuchsin: Lab- and large-scale investigations," *Spectrochimica Acta Part A: Molecular and Biomolecular Spectroscopy*, vol. 306, p. 123621, Feb. 2024, doi: https://doi.org/10.1016/j.saa.2023.123621

[25] M. Abbas, S. Mohammed Al-Hermizy, Z. Abudi, and T. Ibrahim, "Phenol Biosorption from Polluted Aqueous Solutions by Ulva Lactuca Alga Using Batch Mode Unit," *J. Ecol. Eng.*, vol. 20, no. 6, pp. 225–235, Jun. 2019, doi: https://doi.org/10.12911/22998993/109460

[26] Z. Ibrahim *et al.*, "Adsorption of Pyridine onto Activated Montmorillonite Clays: Effect Factors, Adsorption Behavior and Mechanism Study," *AJAC*, vol. 09, no. 10, pp. 464–481, 2018, doi: https://doi.org/10.4236/ajac.2018.910035

[27] A. G. Yewale, N. D. Patil, and A. W. Patwardhan, "Removal of pyridine from dilute aqueous streams using hollow fiber supported liquid membranes," *Desalination and Water Treatment*, vol. 57, no. 40, pp. 18939–18955, Aug. 2016, doi: https://doi.org/10.1080/19443994.2015.1093550

[28] E. García-Hernández *et al.*, "3D Modeling of the Adsorption Rate of Pyridine on Activated Carbon Cloth in a Stirred Tank under Turbulent Conditions," *Processes*, vol. 10, no. 4, p. 735, Apr. 2022, doi: https://doi.org/10.3390/pr10040735

[29] H. Xu *et al.*, "Removal of Pyridine from Aqueous Solutions Using Lignite, Coking Coal, and Anthracite: Adsorption Kinetics," *Processes*, vol. 11, no. 11, p. 3118, 2023, doi: https://doi.org/10.3390/pr11113118.

[30] M. Xia, C. Jin, X. Kong, M. Jiang, D. Lei, and X. Lei, "Green removal of pyridine from water via adsolubilization with lignosulfonate intercalated layered double hydroxide," *Adsorption Science & Technology*, vol. 36, no. 3–4, pp. 982–998, May 2018, doi: https://doi.org/10.1177/0263617417737642

[31] R. Duan, C. B. Fedler, and X. Jiao, "Adsorption of pyridine from aqueous solutions onto polyaluminium chloride and anionic polyacrylamide water

treatment residuals," *Water Science and Technology*, vol. 83, no. 7, pp. 1753–1763, Apr. 2021, doi: https://doi.org/10.2166/wst.2021.082

[32] M. Hamayun *et al.*, "Adsorption of a highly toxic aromatic pollutant from aqueous solution using low cost activated carbon: Equilibrium, kinetic and thermodynamic aspects," *Chiang Mai Journal of Science*, vol. 45, no. 3, pp. 1471–1485, May 2018. [Online]. Available: https://epg.science.cmu.ac.th/ejournal/journal-detail.php?id=9154

[33] Z. A. Jadooa, A. A. Alsarayreh, and M. N. Abbas, "Adsorption of thallium using tangerine peels and exploitation from the waste in an eco-friendly manner," *Ecol. Eng. Environ. Technol.*, vol. 26, no. 2, pp. 131–152, Feb. 2025, doi: https://doi.org/10.12912/27197050/196880

[34] D. Mohan, K. P. Singh, S. Sinha, and D. Gosh, "Removal of pyridine from aqueous solution using low cost activated carbons derived from agricultural waste materials," *Carbon*, vol. 42, no. 12–13, pp. 2409–2421, 2004, doi: https://doi.org/10.1016/j.carbon.2004.04.026

[35] D. H. Lataye, I. M. Mishra, and I. D. Mall, "Pyridine sorption from aqueous solution by rice husk ash (RHA) and granular activated carbon (GAC): parametric, kinetic, equilibrium and thermodynamic aspects," *Journal of Hazardous Materials*, vol. 154, no. 1–3, pp. 858–870, 2008, doi: https://doi.org/10.1016/j.jhazmat.2007.10.111

[36] V. Gosu, B. R. Gurjar, R. Y. Surampalli, and T. C. Zhang, "Treatment of pyridine-bearing wastewater by nano zero-valent iron supported on activated carbon derived from agricultural waste," *Desalination and Water Treatment*, vol. 57, no. 14, pp. 6250–6260, 2016, doi: https://doi.org/10.1080/19443994.2015.1005686